Hydrogen Peroxide Decomposition in Supercritical Water

Eric Croiset, Steven F. Rice, and Russell G. Hanush
Combustion Research Facility, Sandia National Laboratories, Livermore, CA 94551

This work determines the rate constant of hydrogen peroxide decomposition in supercritical water. Experiments were conducted at pressures ranging from 5.0 to 34.0 MPa and for temperatures up to 450°C. The rate of the homogeneous decomposition reaction is distinguished from the rate of the catalytic decomposition on the reactor surface by conducting experiments at different surface-to-volume ratios. The rate constant of H_2O_2 decomposition follows the expression $k(s^{-1}) = 10^{13.4 \pm 1.2} \exp[(-180 \pm 16$ kJ/mol)/RT], providing a higher value than that derived from RRKM calculations. Comparison between experiments at supercritical conditions ($P = 24.5$ and 34.0 MPa) and experiments in high-pressure steam ($P = 5.0$ and 10.0 MPa) show that the efficiency of the catalytic surface reactions decreases significantly under supercritical conditions. The rate constant just mentioned was incorporated into a methanol oxidation model and the new prediction is compared with the experimental data of Rice et al. (1996), showing a distinct improvement compared to the original prediction.

Introduction

Supercritical water oxidation (SCWO), a form of hydrothermal oxidation (HTO) processing, is a promising alternative technology for the destruction of hazardous waste. Above its critical point (374°C and 22.1 MPa), water has properties such that organic compounds oxidize rapidly in a single phase to form products such as CO_2 and H_2O. Over the past few years, there has been considerable effort to characterize the rate of the destruction of different hydrocarbons by this process (Webley and Tester, 1991; Hirth and Franck, 1993; Holgate and Tester, 1994a,b; Alkam et al., 1996; Steeper et al., 1996; Brock and Savage, 1995). Kinetics modeling in several of the articles just mentioned points out the high sensitivity of organic oxidation to hydrogen peroxide decomposition:

$$H_2O_2 + (M) \rightarrow 2\,OH + (M), \qquad \text{(R1)}$$

where the collision partner, M, is water. Unfortunately, experimental data available for this reaction are either in the gas phase (Giguère and Lu, 1957; Meyer et al., 1969) or in the aqueous phase for temperatures below 280°C (Takagi and Ishigure, 1985). No direct measurements of the reaction rate of hydrogen peroxide decomposition in supercritical water conditions are available in the literature.

For purposes of elementary modeling for high-pressure hydrothermal oxidation, this reaction rate has been determined by means of RRKM calculations with an assessment of the high-pressure limit (Holgate, 1993). Using a calculated rate constant, elementary models have succeeded fairly well in reproducing experimental data in supercritical water conditions in the case of hydrogen oxidation at 550 and 570°C (Holgate, 1994b) and methanol oxidation (Rice et al., 1996). Yet, in the work of Rice et al., the predicted conversion of methanol for temperatures below 490°C appears to be slower than the conversion given by the experimental data, with the discrepancies increasing at lower temperatures. Because the dissociation of hydrogen peroxide was found to be rate controlling in the elementary reaction model during much of the reaction of methanol oxidation, the principal cause of discrepancy between experimental results and model prediction may likely originate from the rate of H_2O_2 decomposition. On a molecular scale, the nature of H_2O_2 dissociation may be explicitly affected by the presence of water, resulting in additional buffer concentration dependencies not calculable by way of the RRKM method.

Correspondence concerning this article should be addressed to S. F. Rice.

The present work determines the rate constant of hydrogen peroxide decomposition by direct measurements in a supercritical flow reactor, for pressures ranging from 5.0 MPa to 34.0 MPa and for temperatures up to 450°C. In order to determine the homogeneous dissociation of H_2O_2 independent of catalytic dissociation occurring on the reactor surface, experiments were conducted in reactors of different surface-to-volume (S/V) ratios. An experimentally determined expression for the homogeneous dissociation of H_2O_2 is derived and incorporated into a methanol oxidation model. The new prediction is compared with the experimental data of Rice et al. (1996), showing a distinct improvement compared to the original prediction.

Experimental Section

The hydrogen peroxide decomposition experiments presented here were conducted in Sandia's Supercritical Fluids Reactor (SFR), described in detail elsewhere (Hanush et al., 1995; Rice et al., 1996). For the present work, several modifications were made from the previous configuration, and consequently, a brief description of the main characteristics of the reactor is warranted here.

The reactor is fed by two high-pressure lines, one for the primary water stream and the second for hydrogen peroxide. The water-line pressurization consists of a supply tank and a pneumatic high-pressure liquid pump (AE Maximator, PPSF111). The fluid is preheated in a staged subsystem consisting of Inconel 625 high-pressure tubing, 0.48-cm (3/16-in.) ID, totaling a length of 310 cm. The high-pressure pump provides water at a rate varying from 0.15 $mL \cdot s^{-1}$ to 1.0 $mL \cdot s^{-1}$ at STP conditions. The hydrogen peroxide feed system consists of an H_2O_2 supply vessel, an HPLC pump (LDC Analytical, ConstaMetric 3200) and an injector tube of 0.033-cm (0.013-in.) ID. The HPLC pump delivers flow rates varying from 0.001 $mL \cdot s^{-1}$ to 0.16 $mL \cdot s^{-1}$ at STP conditions. Both water and hydrogen peroxide tanks are placed on electronic balances (Mettler PC4400 and PE300, respectively) and their mass variations are followed during the experiments. This leads to higher accuracy for flow-rate measurement and can identify cavitation problems in the HPLC pump that occasionally occur when working at high H_2O_2 concentration. Hydrogen peroxide feed is prepared by adding the appropriate mass of deionized water to 30 wt. % H_2O_2 (J. T. Baker, electronic grade). Hydrogen peroxide and water are mixed under turbulent conditions in a 10.2-cm opposed-flow tee mixer. Hydrogen peroxide is preheated to the reaction temperature prior to mixing in the final section of the injector located within the tee fitting. Nonisothermal decomposition in the injector is negligible for temperatures below 300°C, but becomes very important for temperatures above 380°C and is addressed below. The combined flows then pass into the reactor subsystem that, similar to the preheater, consists of 0.48-cm (3/16-in.) ID tubing. Samples are collected at several points along the length of the reactor. The sampling line is a 0.015-cm (0.006-in.) ID tube and is immediately cooled by immersion in a water bath. The approximate calculated quench time of 10 ms represents less than 1% of the total reaction time. Samples are analyzed after collection by iodometric analysis. In addition, for concentrations less than 4 ppm (weight basis) hydrogen peroxide content is measured by photoelectric colorimetric analysis (Orbeco-Hellige, Water Analyzer Model 943). With this method, hydrogen peroxide concentrations as low as 0.02 ppm can be measured.

In order to determine reaction rates, residence time must be determined, which in turn requires the density and the mass flow rate of the fluid. At constant mass flow rate, the density of the fluid changes as the reaction proceeds due to the change in composition of the system from an H_2O-H_2O_2 binary mixture to an H_2O-O_2-H_2O_2 ternary mixture. The maximum initial H_2O_2 concentration at the mixing point was only 4% mole fraction and the hydrogen peroxide decomposition rate is sufficiently fast in the supercritical phase that H_2O_2 was present in only small amounts in the reactor. The density of the final mixture, essentially water and oxygen, is then a reasonable approximation of the density of the fluid throughout the reactor. The residence time in the reactor is calculated from the density of the final mixed stream, an H_2O-O_2 binary mixture. The density of the final mixture is determined from an equation-of-state (EOS) calculation proposed by Gallagher et al. (1993a) for mixtures of gases and supercritical water. Calculated results on the H_2O-CO_2 system (Gallagher et al., 1993a) and the H_2O-N_2 system (Gallagher et al., 1993b), with which this EOS formulation was tested, produce an uncertainty in the density estimated to be less than 2%. For the H_2O-O_2 system, the species-specific parameters required by the program were obtained by comparison to the data of Japas and Franck (1985). The uncertainty for the H_2O-O_2 system is very likely to be also on the order of 2%. Mass flow rates were determined directly from the electronic balance data as a function of time. With this method the mass flow rates are known to within $\pm 0.5\%$.

Results and Discussion

Rate constant derivations

Global kinetics of hydrogen peroxide decomposition are assumed to follow first-order reaction kinetics:

$$-\frac{d[H_2O_2]}{dt} = k_g[H_2O_2], \tag{1}$$

where $[H_2O_2]$ is the hydrogen peroxide molar concentration, and k_g is the global H_2O_2 decomposition rate constant, in s^{-1}. The rate constant is defined in terms of the experimental measurements by integrating Eq. 1 to yield

$$\ln\left(\frac{[H_2O_2]_f}{[H_2O_2]_i}\right) = -k_g t, \tag{2}$$

where t is the residence time and where the index i represents the initial concentration and the index f represents the measured final concentration. Ordinarily, in our SFR reactor configuration, the initial concentration of hydrogen peroxide is the concentration at the mixing point. Unfortunately, the hydrogen peroxide concentration at the mixing point is not known due to wall-catalyzed decomposition inside the small ID injector. As a result, Eq. 2 must be written in terms of the known concentration in the H_2O_2 supply vessel, rather than the poorly defined concentration at the mixing point. Equation 2 is then rewritten in the following form:

$$\ln\left(\frac{[H_2O_2]_f}{[H_2O_2]_0}\right)+\ln\left(\frac{[H_2O_2]_0}{[H_2O_2]_1}\right)+\ln\left(\frac{[H_2O_2]_1}{[H_2O_2]_i}\right)=-k_g t, \tag{3}$$

where $[H_2O_2]_0$ represents the molar concentration inside the H_2O_2 supply vessel, and $[H_2O_2]_1$ is the hydrogen peroxide concentration at the end of the injector just after the mixing point. The first and third terms on the lefthand side of Eq. 3 are equal to

$$\ln\left(\frac{[H_2O_2]_f}{[H_2O_2]_0}\right)=\ln\left(\frac{\rho_f W_f}{\rho_0 W_0}\right) \tag{4}$$

and

$$\ln\left(\frac{[H_2O_2]_1}{[H_2O_2]_i}\right)=\ln\left(\alpha\frac{\rho_1}{\rho_i}\right), \tag{5}$$

where α is a dilution factor equal to $(F_{hp}+F_w)/F_{hp}$, with F_{hp} and F_w representing the hydrogen peroxide and water mass flow rates, respectively; ρ is the total density; and W is the hydrogen peroxide mass fraction. With the assumption that $\rho_1 \approx \rho_i \approx \rho_f$, Eq. 3, combined with Eqs. 4 and 5, becomes

$$\ln\left(\alpha\frac{\rho_f}{\rho_0}\frac{W_f}{W_0}\right)=\ln\left(\frac{[H_2O_2]_f}{[H_2O_2]_i'}\right)=-k_g t+\ln\left(\frac{[H_2O_2]_1}{[H_2O_2]_0}\right). \tag{6}$$

The lefthand side of Eq. 6 is determined experimentally. The plot of $\ln[\alpha\rho_f W_f/(\rho_0 W_0)]$ vs. time is then a linear function with a slope that represents the rate constant. Here, the concentration $[H_2O_2]_i'$ is the exact value of the initial concentration in the absence of hydrogen peroxide decomposition inside the injector. Without this decomposition the graph obtained from the relationship represented by the lefthand side of Eq. 6 vs. time is a straight line passing through the origin. Because of decomposition in the injector, a nonzero y-intercept is realized.

Experimental measurements

The first set of measurements were aimed at determining the global hydrogen peroxide decomposition rate constant. As will be seen later, this global rate includes homogeneous decomposition and decomposition due to catalysis by the reactor surface. By conducting specific experiments described below that vary the system S/V ratio, the wall-catalyzed decomposition rate can be separated from the homogeneous process. The rate constants due to wall surface and to homogeneous reactions are treated in the following "Surface Effects" section. This section addresses only the determination of the global rate constants.

Experiments were performed at 24.5 and 34.0 MPa for temperatures ranging from 150°C to 450°C. Figures 1 and 2 show the plots of $\ln[(H_2O_2]_f/[H_2O_2]_i')$ vs. residence time at 24.5 MPa, for temperatures below and above the critical temperature of water (374°C). The curves obtained are straight lines, which confirms that the decomposition of hydrogen

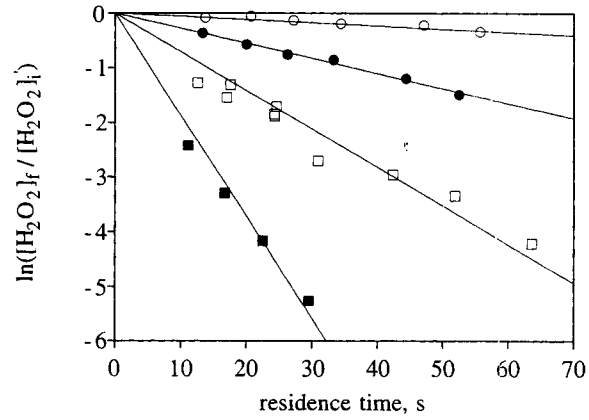

Figure 1. Variation of $\ln([H_2O_2]_f/[H_2O_2]_i')$ vs. residence time.

Pressure = 24.5 MPa. Results are shown for temperatures below the critical temperature of water: 150°C ○; 200°C ●; 250°C □; 300°C ■.

peroxide follows first-order global kinetics. Comparison between these two figures shows important differences between experiments conducted above and below the critical temperature of water, T_c (374°C). For experiments well below T_c, the straight lines pass through the origin, indicating no significant H_2O_2 decomposition inside the injector, whereas near and above T_c, the straight lines do not pass through the origin, implying considerable H_2O_2 decomposition before the mixing point. However, H_2O_2 decomposition inside the injector does not prevent the interpretation of the results, because Eq. 6 shows that only the slope of the curve is necessary to determine the rate constant in the larger bore reactor. At 34.0 MPa the plots obtained are very similar to those at 24.5 MPa. All rate constants, at different pressures and temperatures, are given in Table 1.

The Arrhenius plots at 24.5 and 34.0 MPa are presented in Figure 3. This figure shows no measurable differences between 24.5 and 34.0 MPa below or above the critical temperature of water. Below 374°C, straight lines confirm that the

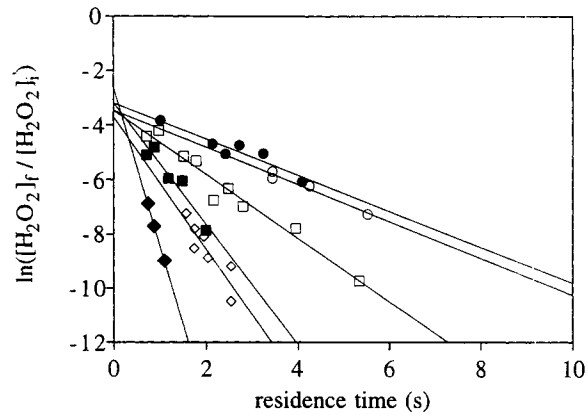

Figure 2. Variation of $\ln([H_2O_2]_f/[H_2O_2]_i')$ vs. residence time.

Pressure = 24.5 MPa. Results are shown for temperatures above the critical temperature of water: 380°C ○; 390°C ●; 400°C □; 420°C ■; 425°C ◇; and 440°C ◆.

Table 1. Global First-Order Rate Constants for Hydrogen Peroxide Decomposition at 34.0, 24.5, 10.0 and 5.0 MPa, at Temperatures Ranging from 150°C to 450°C

P (MPa)	T (°C)	k_g (s^{-1})	P (MPa)	T (°C)	k_g (s^{-1})
34.0	180	0.02±0.002	24.5	400	1.17±0.09
34.0	250	0.11±0.005	24.5	420	2.22±0.39
34.0	300	0.20±0.002	24.5	425	2.42±0.57
34.0	350	0.46±0.02	24.5	440	5.80±0.22
34.0	380	0.48±0.02	10.0	330	2.73±0.19
34.0	400	0.62±0.05	10.0	350	2.51±0.35
34.0	425	2.00±0.41	10.0	370	2.73±0.29
34.0	440	3.84±0.41	10.0	390	3.57±0.17
34.0	450	5.88*	10.0	410	4.20*
24.5	150	0.01±0.000	5.0	160	0.01±0.000
24.5	200	0.03±0.000	5.0	200	0.03±0.001
24.5	250	0.07±0.003	5.0	230	0.05±0.002
24.5	300	0.19±0.006	5.0	280	2.31±0.32
24.5	380	0.68±0.10	5.0	300	2.34±0.65
24.5	390	0.66±0.11	5.0	320	3.08±0.42

*Error on k not determined, only two data points.

rate constant follows the Arrhenius form. Above 374°C, the plot at 34.0 MPa is also a straight line with a slight curvature at the lower temperatures. At 24.5 MPa, the plot presents a slightly more pronounced curvature that is more easily observed at temperatures below 420°C. However, above 420°C, the plot converges with the plot for the 34.0 MPa data. The data at 34.0 MPa fall in two straight lines, with a break in the slope occurring near the critical temperature of water, indicating that the activation energy in the supercritical region is much higher than in the liquid water phase. The regressed expressions of the rate constants are, in the temperature range 150–450°C, liquid phase ($T < 374$°C, $P = 5$–34 MPa):

$$k_g = 10^{3.5 \pm 0.2} \exp[(-46 \pm 2 \text{ kJ/mol})/RT] \quad (s^{-1}) \quad (7)$$

and in the supercritical phase ($T > 380$°C, $P = 24.5$–34 MPa):

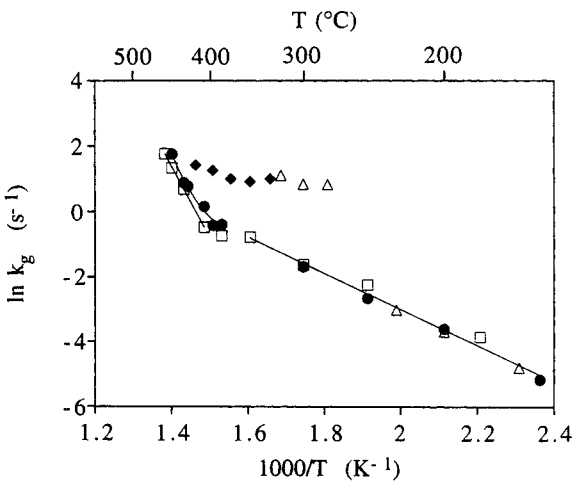

Figure 3. Arrhenius plot of ln (k_g) vs. the reciprocal of the temperature.

The global rate constants were determined experimentally from the raw data (for example, from Figure 2 at 24.5 MPa). The lines are linear fits to data and the curves are polynomial fits to data: 5.00 MPa ◆; 10.0 MPa △; 24.5 MPa ●; and 34.0 MPa □.

$$k_g = 10^{13.9 \pm 0.07} \exp[(-182 \pm 1 \text{ kJ/mol})/RT] \quad (s^{-1}). \quad (8)$$

In addition, a series of experiments was performed at 5.0 and 10.0 MPa to investigate the behavior of H_2O_2 decomposition below the critical pressure of water (22.1 MPa). The results are also shown in Figure 3. In the liquid phase (for example, $T < 260$°C at 5.0 MPa), the rate constant is identical to the liquid-phase values at 24.5 and 34.0 MPa. This can be explained by the fact that water density varies only slightly with pressure in the liquid phase. For example, at 240°C, water density changes from 815 $kg \cdot m^{-2}$ at 5.0 MPa to 841.9 $kg \cdot m^{-2}$ at 34.0 MPa (NBS Steam Tables, Haar et al., 1984). In the gas phase, the Arrhenius plot at 5.0 and 10.0 MPa is much different from the plots under supercritical conditions. The observed rate constants appear to be very weakly dependent on temperature below 370°C and an increase in the rate constant occurs for temperatures above 370°C. However, none of the curves obtained at 5.0 and 10.0 MPa in the gas phase follow an Arrhenius form. This observed deviation from an expected Arrhenius behavior originates from surface reactions effects and will be treated below.

Surface-effects measurements

The rate of decomposition of hydrogen peroxide on surfaces is known to be sensitive to the surface properties (Cheaney et al., 1959; Hart et al., 1963; Hoare et al., 1967). Surface effects may be important here and thus may impact significantly the value of the overall rate constant measured experimentally. To investigate this, experiments were performed at different values of S/V ratios. The original reactor, in which the experiments described earlier were conducted, has an S/V ratio of 8.33 cm^{-1}. To obtain a higher S/V ratio, seven 0.16-cm OD (1/16-in.) Inconel 625 tubes were introduced in the 3/16-in. ID original reactor, such that one tube was positioned in the center of the reactor and the other six surrounded it. The S/V ratio thus obtained is 55.5 cm^{-1}, corresponding to almost a sevenfold increase. Using this method, the surface of the reactor is increased significantly by adding smaller tubes, while the reactor volume decreased only slightly (less than a factor of 1.5 in this case). The dominant change from the previous experiments is then only in the S/V ratio. These experiments were conducted at 24.5 MPa and at temperatures ranging from 300°C to 420°C.

Figure 4 shows the influence of the S/V ratio on the rate constant, when the ratio is increased from 8.3 cm^{-2} to 55.5 cm^{-1}. This figure indicates that the slopes, and thus the rate constants, are influenced by an increase in the S/V ratio. For example, at 410°C, k increases from 1.4 s^{-1} (at S/V = 8.3 cm^{-1}) to 2.9 s^{-1} (at S/V = 55.5 cm^{-1}). The true homogeneous hydrogen peroxide decomposition rate constant corresponds to the experimental rate constant when the S/V ratio approaches zero. By assuming that the observed rate constant varies linearly with the S/V ratio, extrapolation to zero S/V will give the homogeneous decomposition rate constant (Holgate and Tester, 1994a). Analytically, this method leads to the following expression:

$$k = k_h + k_w\left(\frac{S}{V}\right) \quad (9)$$

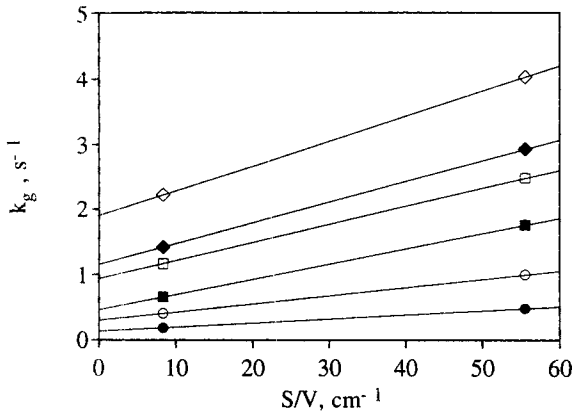

Figure 4. Influence of the surface-to-volume ratio on the global decomposition rate constant for the hydrogen peroxide.

The values for k_g are the observed global rate constants for the decrease in H_2O_2 determined from fits to $k_g = -d \ln [H_2O_2]/dt$. Pressure = 24.5 MPa. The different temperatures are: 300°C ●; 350°C ○; 390°C ■; 400°C □; 410°C ◆; 420°C ◇.

where k_h and k_w are rate constants, respectively, for the homogeneous decomposition and for the catalytic decomposition on the wall. The global heterogeneous decomposition rate can thus be determined as follows:

$$k_w\ (\mathrm{cm \cdot s^{-1}}) = \frac{(k)_1 - (k)_2}{\left(\frac{S}{V}\right)_1 - \left(\frac{S}{V}\right)_2}, \tag{10}$$

where the indices 1 and 2 represent, respectively, experiments run in the reactor with low and high S/V ratios. The data show that, at supercritical water conditions, k_w follows the Arrhenius form and the following expressions were determined by linear regression:

$$k_w = 10^{3.3 \pm 0.3} \exp[(-62.5 \pm 4.4\ \mathrm{kJ/mol})/RT] \quad \text{for } T \geq T_c \tag{11}$$

$$k_w = 10^{1.5} \exp[(-40.8\ \mathrm{kJ/mol})/RT] \quad \text{for } T < T_c. \tag{12}$$

Finally, knowing k_w, the homogeneous rate constant is found to be equal to

$$k_h = 10^{13.7 \pm 1.2} \exp[(-180 \pm 16\ \mathrm{kJ/mol})/RT] \quad \text{for } T > 380°C \tag{13}$$

$$k_h = 10^{3.6 \pm 0.3} \exp[(-49 \pm 3\ \mathrm{kJ/mol})/RT] \quad \text{for } T < 350\ °C. \tag{14}$$

After correction for the surface effect, the rate constant of homogeneous H_2O_2 decomposition in the supercritical water region at 24.5 MPa (see Eq. 13) agrees very well with the expression found at 34.0 MPa (see Eq. 8). We conclude that the rate constant in the supercritical water region is thus pressure independent. The rate constant k_w represents only about 20% of the global rate constant, and appears to have a decreasing influence at higher temperature relative to the homogeneous term. In fact, the normally configured reactor S/V ratio is sufficiently small to require only a minor extrapolation from the global rate to the homogeneous rate. The magnitude of this correction is near the experimental accuracy.

In the liquid phase, the rate constant described by Eq. 14 is very similar to the one without correction from the wall surface, implying that wall surface does not alter significantly the global rate constant in the liquid phase, again reflecting a decreased influence of surface reactions at higher fluid densities.

Reaction mechanism of H_2O_2 decomposition

Models based on global kinetics do not provide the same predictive capability as models based on verified elementary reaction schemes. The purpose of this section is to determine the rate constant of the elementary reaction of H_2O_2 dissociation, which as will be seen, can be derived from the measured homogeneous rate constant. Earlier, hydrogen peroxide decomposition was described by the decomposition reaction

$$H_2O_2 \xrightarrow{k_h} H_2O + 1/2\ O_2. \tag{15}$$

It has been suggested (Giguère and Liu, 1957; Tagaki and Ishigure, 1985) that this reaction proceeds by the pathway:

$$H_2O_2 + (M) \xrightarrow{k_1} 2\ OH + (M) \tag{R1}$$

$$OH + H_2O_2 \xrightarrow{k_2} H_2O + HO_2 \tag{R2}$$

$$OH + HO_2 \xrightarrow{k_3} H_2O + O_2 \tag{R3}$$

$$HO_2 + HO_2 \xrightarrow{k_4} H_2O_2 + O_2. \tag{R4}$$

The collision partner in reaction R1 is H_2O, which is in large excess. Moreover, the parentheses surrounding the collision partner in reaction R1 indicate that at lower pressures the rate for hydrogen peroxide unimolecular dissociation requires a collision. For the densities in the supercritical region, RRKM calculations indicate (Tsang and Hampson, 1986) that the reaction rate is in the high-pressure limit and that an increased frequency of collisions does not increase the rate. This hypothesis is strengthened by the results of experiments of Meyer et al. (1969), who observed that the high-pressure falloff region begins at about 2.0 MPa. In addition, rate constants data obtained at 24.5 and 34.0 MPa (see Figure 3) show that these rate constants are independent of the pressure, supporting the fact that the reaction rate is at the high-pressure limit in the supercritical region. Under the conditions of the present work, the collision partner in reaction R1 is thus omitted.

According to reactions R1–R4, the expression of the rate of disappearance of $[H_2O_2]$ is written as:

Table 2. Different Values for H_2O_2 Thermal Decomposition Rate Constants*

	log A	E (kJ mol^{-1})	Temp. range (°C)	Remarks
		Supercritical Region		
This work	13.4±1.2	180±16	380–450	P = 24.5–34.0 MPa
Holgate (1993)	14.9	209	400–600	P = 24.6 MPa
		Vapor Phase		
Giguère and Liv (1957)	13.0	201	400–500	$P = 3\times10^{-5}$–3×10^{-3} MPa
Meyer et al. (1969)	13.5	207	677–1177	$k = k_\infty$
Baulch et al. (1994)	14.5	203	730–1230	$k = k_\infty$
		Aqueous Phase		
This work	3.6±0.3	49±3	150–350	P = 5, ..., 34 MPa
Takagi and Ishigure (1985)	5.8	71	100–250	At least up to 4 MPa**

*These values are given for different states of water. The rate constant k is of the form $k = A\exp(-E/RT)$. k_∞ accounts for the high-pressure, second-order limit.
**Maximum operating pressure estimated from water vapor pressure at 250°C.

$$\frac{d[H_2O_2]}{dt} = -k_1[H_2O_2] - k_2[OH][H_2O_2] + k_4[HO_2]^2. \quad (16)$$

Using the steady-state assumption for [OH] and [HO_2] we obtain

$$\frac{d[H_2O_2]}{dt} = -2k_1[H_2O_2], \quad (17)$$

which indicates that the rate measured experimentally is twice the elementary first-order rate constant for reaction R1. The assumption of steady-state for [OH] and [HO_2] was examined using the detailed mechanism for the H-O system and is discussed at the end of this section.

From our data, in the supercritical region the rate constant k_1 becomes

$$k_1 = 10^{13.4\pm1.2}\exp[(-180\pm16\ \text{kJ/mol})/RT]. \quad (18)$$

Likewise, in the aqueous phase, the rate constant k_1 is

$$k_1 = 10^{3.3\pm0.3}\exp[(-49\pm3\ \text{kJ/mol})/RT]. \quad (19)$$

These values are compared in Table 2 with different rate constants found in the literature.

In the aqueous phase the Arrhenius parameters found in the present work are different from those found by Takagi and Ishigure (1985). Yet, the lower activation energy found in this study is counterbalanced by a higher preexponential factor. For these two works, the absolute values of the rate constant are found to be of the same order of magnitude in the temperature range 150–350°C. Our results can then be considered to be in a reasonable agreement with those of Takagi and Ishigure in the aqueous phase.

Considering the state of water in the supercritical region as dense gas, it is meaningful to compare our rate constants in the supercritical region with the high-pressure-limit rate constants in the vapor phase determined by others. This comparison is shown in Figure 5, where each expression is represented in its temperature range. The commonly accepted expression for the gas-phase rate constant is the one recommended by Baulch et al. (1994). The rate constant of Holgate (1993) at 24.6 MPa was determined from RRKM calculations and was found to be very close to the high-pressure limit. The expression derived by Holgate is in fact very close to the expression of Baulch et al. and represents an extrapolation of Baulch values to the temperature range 400–600°C. Therefore, the rate constants of Meyer et al. (1969) are an estimated lower limit of k_∞, and the rate constant of Giguère and Liu (1957), determined at pressures below 3 kPa, was well below the high-pressure limit. Therefore, the values of Meyer and Giguère represent a lower estimate of the hydrogen peroxide decomposition rate constant in their temperature range.

The rate constant determined in the present work, $k_1 = 10^{13.4}\exp(-180{,}000/RT)$, has an error limit, $\Delta \log k_1$, equal to 0.1. By extrapolating the expression of Baulch et al. (1994), whose error limit is 0.5, to 450°C, it is found that $\log k_1$ ranges

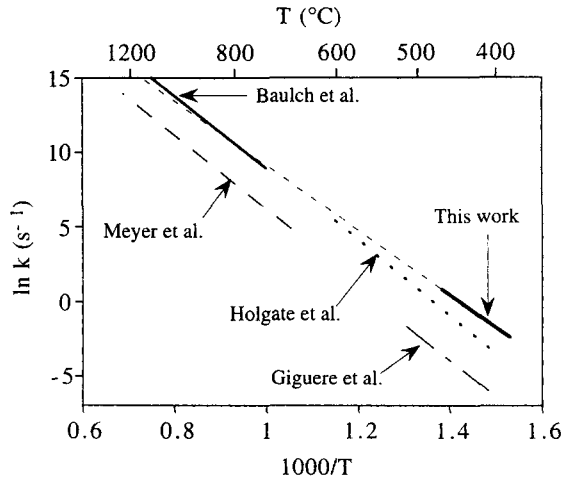

Figure 5. Comparison between different values of rate constants for H_2O_2 thermal decomposition.

Each line is drawn for its corresponding temperature range, except for the thin dashed line, which represents the extrapolation of the present work at higher temperatures. Holgate's work and the present work correspond to supercritical conditions. The rate constants suggested by Baulch et al. and Meyer et al., correspond to the high-pressure limit, k_∞.

Table 3. Detailed Reaction Mechanism for the System O-H*

	Reactions	A	β	T^*	Source
1	$O+H+H_2O\langle=\rangle OH+H_2O$	$4.71E+18$	−1.00	0.0	1
2	$O+H_2\langle=\rangle H+OH$	$5.13E+04$	2.67	3,160.0	2
3	$H+O_2\langle=\rangle O+OH$	$9.75E+13$	0.00	7,470.0	3
4	$O+HO_2\langle=\rangle OH+O_2$	$1.75E+13$	0.00	−200.0	1
5	$O+H_2O_2\langle=\rangle OH+HO_2$	$9.63E+06$	2.00	2,000.0	1
6	$2H+H_2\langle=\rangle 2H_2$	$9.78E+16$	−0.60	0.0	3
7	$H+2O_2\langle=\rangle HO_2+O_2$	$6.41E+18$	−1.00	0.0	1
8	$H+O_2+H_2O\langle=\rangle HO_2+H_2O$	$9.42E+18$	−0.76	0.0	4
9	$H+OH+M\langle=\rangle H_2O+M$	$2.21E+22$	−2.00	0.0	1
10	$H+HO_2\langle=\rangle O+H_2O$	$3.01E+13$	0.00	866.0	3
11	$H+HO_2\langle=\rangle O_2+H_2$	$4.27E+13$	0.00	710.0	3
12	$H+HO_2\langle=\rangle 2OH$	$1.69E+14$	0.00	440.0	3
13	$H+H_2O_2\langle=\rangle HO_2+H_2$	$1.69E+12$	0.00	1,890.0	3
14	$H+H_2O_2\langle=\rangle OH+H_2O$	$1.02E+13$	0.00	1,800.0	3
15	$H_2+H_2O\langle=\rangle 2H+H_2O$	$8.43E+19$	−1.10	52,530.0	1
16	$OH+H_2\langle=\rangle H+H_2O$	$2.16E+18$	1.51	1,726.0	5
17	$2OH\langle=\rangle O+H_2O$	$1.52E+09$	1.14	50.0	3
18	$OH+HO_2\langle=\rangle H_2O+O_2$	$2.89E+13$	0.00	−250.0	3
19	$OH+H_2O_2\langle=\rangle HO_2+H_2O$	$7.83E+12$	0.00	670.0	3
20	$2HO_2\langle=\rangle H_2O_2+O_2^{**}$	$5.28E-35$	14.06	−9,605.0	6
21a	$H_2O_2\langle=\rangle OH+OH^{\dagger}$	$2.28E+13$	0.00	21,650.0	7
21b	$H_2O_2\langle=\rangle OH+OH$	$3.00E+14$	0.00	24,400.0	3
22	$H_2O_2 \xrightarrow{\text{wall}} H_2O+1/2\,O_2$	$1.3E-02\times(S/V)^{\dagger\dagger}$	0.50	0.0	7

*Mechanism applied here in the case of hydrogen peroxide decomposition. Rate constant = $AT^{\beta}\exp(-T^*/T)$ (units of mol, cm^3, s, K).
**Simplified rate form in the temperature range 673–773.
†Determined in supercritical water conditions.
††In the present work, $S/V = 8.33\ cm^{-1}$.
Sources: (1) Tsang and Hampson (1986); (2) Sutherland et al. (1986); (3) Baulch et al. (1994); (4) GRI-Mech 1.2; (5) Michael and Sutherland (1988); (6) Hippler et al. (1990); (7) this work. The species thermochemistry data are those from the GRI mechanism.

from −0.68 to 0.32. A similar calculation using the expression k_1 determined in the present work, shows $\log k_1$ ranging from 0.29 to 0.45. There is only a slight overlap between the values of k_1 derived from the Baulch expression and those from the expression of this work, indicating that the rate constants determined in the present work are measurably higher than the values determined by extrapolation of the Baulch expression, to the temperature range of 380–450°C. The effect of the wall surface was taken into account in the experimental determination of the rate constant, and thus cannot explain the difference between rate constants experimentally determined in the present work and those calculated from RRKM theory. This suggests that, on a molecular scale, the nature of H_2O_2 dissociation may be explicitly affected by the presence of water, resulting in additional buffer concentration dependencies not calculable by way of the RRKM method, at least in the vicinity of the critical point of water. However, extrapolation of the expression found in the present work to the temperature range valid for the Baulch expression gives good agreement between our values and those recommended by Baulch et al., as seen in Figure 5.

Because the determination of k_1 was based only on the four irreversible reactions R1 to R4, kinetic calculations were performed to check this assumption. Using Chemkin (ideal gas EOS) and Chemkin-Real-Gas (Alkam et al., 1996), calculations were done for different mechanism configurations: (1) the detailed mechanism as shown in Table 3; and (2) a simplified mechanism consisting of only the four reactions (R1 to R4) considered as either reversible or irreversible. The results show that, in all cases, the change in H_2O_2 concentration vs. time is identical up to nine orders of magnitude of conversion, at which point, reversibility in reactions R1–R4 permits establishment of equilibrium. This indicates that, not only are the four irreversible reactions R1 to R4 sufficient to describe the kinetics, but that effects due to a nonideal EOS (Peng-Robinson) are unimportant in the determination of k_1.

The determination of k_1 according to Eq. 17 also hypothesizes a steady-state approximation for [OH] and [HO_2]. To check this assumption in the supercritical region, the value of k_1 found in Eq. 18 was incorporated in the mechanism presented in Table 3, and the variation of the natural logarithm of [H_2O_2], [OH], and [HO_2] vs. time is shown in Figure 6. The variation of [OH] vs. time is negligible, and thus the steady-state assumption for OH is valid. The concentration

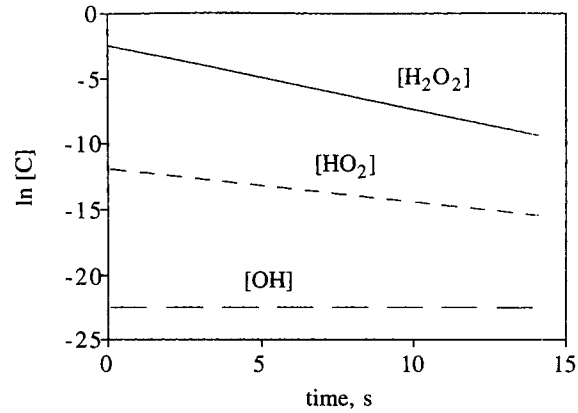

Figure 6. Evolution vs. time of the logarithm of [H_2O_2], [HO_2], and [OH] concentrations; calculation done from the mechanism presented in Table 3.

of $[HO_2]$ decreases with time somewhat, implying that HO_2 does not follow the steady-state assumption. Yet, the slope of the straight line, ln $[H_2O_2]$ vs. time, is still twice the value of k_1, indicating that Eq. 17 is satisfied. In fact, in the temperature range considered here, reaction R3 is negligible compared to reaction R4. Considering only reactions R1, R2, R4, and invoking the steady-state assumption only for OH, yields:

$$\frac{d}{dt}([H_2O_2]+1/2[HO_2]) = -2k_1[H_2O_2]. \qquad (20)$$

Since the concentration of HO_2 is negligible relative to the H_2O_2 concentration, Eq. 20 is equivalent to Eq. 17. Thus Eq. 17 is satisfied, even though the steady-state assumption for HO_2 is not valid.

Surface-effects modeling

In the supercritical region, at 24.5 MPa, it has been seen that surface effects are small but not negligible near T_c in our experimental system. The "Surface-effects Measurements" section shows that the rate constant for the catalytic decomposition on the wall is well approximated by an Arrhenius expression. The Arrhenius parameters were determined accordingly (see Eq. 11).

Simple kinetic theory of gases gives the following expression for the surface reaction rate constant (Hoare et al., 1967):

$$k_w\left(\frac{S}{V}\right) = \Gamma\left(\frac{S}{V}\right)\sqrt{\frac{kT}{2\pi m}}, \qquad (21)$$

where Γ is the efficiency parameter of H_2O_2 removal upon collision with the wall surface, k is the Boltzmann's constant, and m is the mass of an H_2O_2 molecule. Unfortunately, an attempt to fit our data at supercritical conditions to the theoretical expression of Eq. 21 failed. In particular, the temperature dependence of our experimental values of k_w is much greater than can be described by Eq. 21. This suggests that this theoretical expression is not valid at supercritical water conditions for H_2O_2 surface decomposition. Indeed, Eq. 21 is characterized by a relatively weak temperature dependence: k_w is proportional to $T^{1/2}$.

In Figure 3, however, the data shown in the vapor phase at 5.0 and 10.0 MPa do present only a weak temperature dependence. This could be due to a preponderant effect of the surface decomposition over the homogeneous decomposition in the temperature range considered here. To check this possibility, simulation of the gas phase process was done using Arrhenius plots at 5.0 and 10.0 MPa, following the mechanism shown in Table 3 in which the surface-effect rate constant satisfies Eq. 21. The adjustment of the H_2O_2 efficiency parameter to the data at 10.0 MPa leads to the fitted value of $\Gamma_{H_2O_2} = 2.1\times10^{-5}$. From Eq. 21, the reaction rate of the catalytic decomposition of H_2O_2 on the wall is then expressed as:

$$k_w\,(\mathrm{cm\cdot s^{-1}}) = 1.3\times10^{-2}\times T^{0.5}. \qquad (22)$$

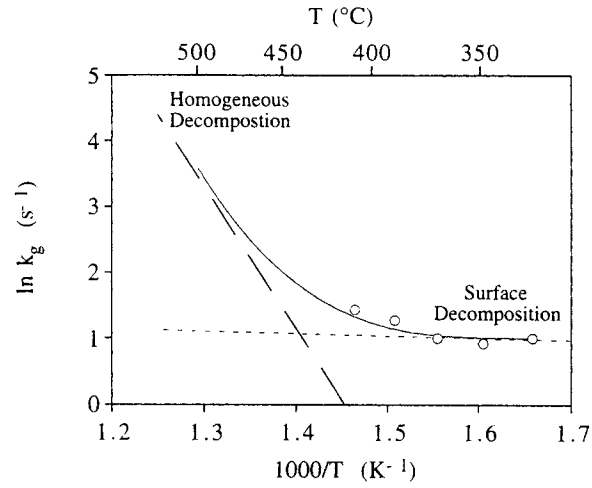

Figure 7. Results from the elementary reaction model in Table 3 vs. the experimental data, Arrhenius plot simulation at 10.0 MPa.

The open symbols represent experimental data, and the solid line represents the calculated values of ln k_g. The dashed line —— represents ln $(2k_1)$ and the dashed line – · – · – represents ln (k_w) according to Eq. 22.

The model was investigated by using the rate constant of homogeneous hydrogen peroxide decomposition (reaction R1) found in the present work under supercritical conditions. Comparison of the experimental values with the calculation is shown in Figure 7. This figure shows the transition between decomposition controlled by the surface effects to decomposition controlled by homogeneous reactions. Figure 7 suggests that, under the conditions examined here, the experimental data at 10.0 and 5.0 MPa reflect essentially hydrogen peroxide decomposition on the wall surface.

Comparison between Eq. 11 and Eq. 22 shows that the wall surface decomposition is much more important in the gas phase than in the higher density supercritical phase. For example, the rate constant of the wall effect, k_w, at 400°C is 0.34 $\mathrm{m\cdot s^{-1}}$ in the vapor phase (at 10.0 MPa) and 0.03 $\mathrm{cm\cdot s^{-1}}$ under supercritical conditions. Apparently, at the higher density supercritical conditions, the efficiency of the inhomogeneous process is significantly lower, perhaps due to significantly slower diffusion to or from the active sites on the wall. It appears that the same homogeneous process occurs over the pressure range from 5 MPa to 34 MPa. However, experimental limitations, especially due to very fast reactions, prevented us from measuring the homogeneous H_2O_2 decomposition rate directly in the vapor phase at higher temperature.

H_2O_2 decomposition and methanol oxidation in SCWO

This research originated from the observation that hydrogen peroxide decomposition plays a key role during the oxidation of methanol in supercritical water (Rice et al., 1996). It was found that the model of Schmitt et al. (1991) reproduces Rice's experimental data fairly well, but predicts rates too slow for temperatures below 490°C. It is also found that, after the induction period, the rate of oxidation of methanol is most sensitive to the rate of the unimolecular dissociation of hydrogen peroxide. We have repeated this calculation with the former expression for the rate of H_2O_2 decomposition

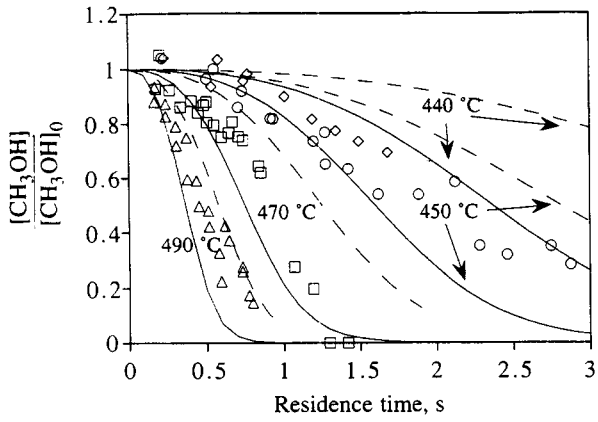

Figure 8. Experimental results for methanol oxidation in supercritical water (Rice et al., 1996) (open symbol) vs. the original model of Schmitt et al. (1991) (dotted lines) and with the same model in which H_2O_2 decomposition rate has been replaced by the value determined in the present work (continuous lines); temperatures: 440°C ◇; 450°C ○; 470°C □; 490°C △.

replaced by the new expression found in the present work. The new prediction of methanol oxidation behavior was then compared with the former prediction and with the experimental data. This comparison is shown in Figure 8. The new values of the H_2O_2 decomposition rate parameters improve the prediction of the model considerably at 440 and 450°C, that is, in the temperature range of the present work. Extrapolations to temperatures above 450°C provide good agreement with the experimental data, although at 470 and 490°C the rate of methanol disappearance is predicted to be slightly too fast.

Conclusions

The decomposition rate of hydrogen peroxide is determined experimentally for pressures ranging from 5.0 to 34.0 MPa and temperatures up to 450°C. It is found that H_2O_2 decomposition in water follows first-order kinetics in the aqueous, vapor, and supercritical phases. The homogeneous dissociation rate of hydrogen peroxide is found to be independent of the dissociation on surfaces of the reactor. The important factor determining the homogeneous rate of hydrogen peroxide thermal decomposition in water is the water density. The catalytic decomposition of H_2O_2 at a surface is also determined and is found to vary with water density; its importance decreases when the density increases. In the liquid phase, where the density is the highest, the influence of surface reactions is small, whereas in the gas phase surface reactions can dominate, especially at low temperatures. Due to higher fluid densities, surface reactions have a smaller effect under supercritical conditions than in the subcritical high-pressure steam phase.

By considering the surface effect, the true homogeneous rate of H_2O_2 decomposition is determined and found to equal $10^{13.4\pm1.2}$ exp[$(-180\pm16$ kJ/mol$)/RT$] in the supercritical region at 24.5 and 34.0 MPa. In the temperature range considered here (380–450°C), this rate leads to values higher than those found from RRKM calculations. In addition, results for experiments conducted in the gas phase at 5.0 and 10.0 MPa reflect essentially the hydrogen peroxide decomposition on the reactor's surface, which allows us to determine the corresponding reaction rate based on a simple theoretical expression derived from the kinetic theory of gases. However, this theoretical expression fails in describing the surface effect in the supercritical region and an empirical Arrhenius-form expression was found to be more relevant. Finally, at supercritical water conditions, and for temperatures below 470°C, the reaction rate for hydrogen peroxide thermal decomposition determined in the present work improves significantly the accuracy of the methanol oxidation model studied by Rice et al. (1996).

Acknowledgments

This work was supported by the DoD/DOE/EPA Strategic Environmental Research and Development Program (SERDP). The first author (E.C.) was sponsored at Sandia by la Région Centre, France. We thank Jessica Wickham (Cornell University) for technical assistance.

Literature Cited

Alkam, M. K., V. M. Pai, P. B. Butler, and W. J. Pitz, "Methanol and Hydrogen Oxidation Kinetics in Water at Supercritical States," *Combust. Flame*, **106**, 110 (1996).

Baulch, D. L., C. J. Cobos, R. A. Cox, P. Frank, G. Hayman, Th. Just, J. A. Kerr, T. Murrells, M. J. Pilling, J. Troe, R. W. Walker, and J. Warnatz, "Evaluated Kinetic Data for Combustion Modelling—Supplement I," *J. Phys. Chem. Ref. Data*, **23**(6), 847 (1994).

Brock, E. E., and P. E. Savage, "Detailed Chemical Kinetics Model for Supercritical Water Oxidation of C_1 Compounds and H_2," *AIChE J.*, **41**(8), 1874 (1995).

Cheaney, D. E., D. A. Davis, A. Davis, J. B. Hoare, J. B. Protheroe, and A. D. Walsh, "Effects of Surfaces on Combustion of Methane and Mode of Action of Anti-knocks Containing Metals," *Int. Symp. on Combust. Proc.*, published by Buttersworth Scientific Publications, London, p. 183 (1959).

Gallagher, J. S., R. Crovetto, and J. M. H. Levelt Sengers, "The Thermodynamic Behavior of the CO_2-H_2O System from 400 to 1,000 K, up to 100 MPa and 30% Mole Fraction of CO_2," *J. Phys. Chem. Ref. Data*, **22**(1), 431 (1993a).

Gallagher, J. S., J. M. H. Levelt Sengers, I. M. Abdulagatov, J. T. R. Watson, and A. Fenghour, "Thermodynamic Properties of Homogeneous Mixtures of Nitrogen and Water from 440 to 1,000 K, up to 100 MPa and 0.8 mole Fraction N_2," NIST Tech. Note 1404, National Institute of Standards and Technology, published by U.S. Government Printing Office, Washington, DC (1993b).

Giguère, P. A., and I. D. Liu, "Kinetics of the Thermal Decomposition of Hydrogen Peroxide Vapor," *Can. J. Chem.*, **35**, 283 (1957).

GRI-Mech 1.2, please refer to this Web page: M. Frenklach, H. Wang, C.-L. Yu, M. Goldenberg, C. T. Bowman, R. K. Hanson, D. F. Davidson, E. J. Chang, G. P. Smith, D. M. Golden, W. C. Gardiner, and V. Lissianski, http://www.gri.org.

Haar, L., J. S. Gallagher, and G. S. Kell, *NBS/NRC Steam Tables: Thermodynamic and Transport Properties and Computer Programs for Vapor and Liquid States of Water in SI Units*, Hemisphere, New York (1984).

Hanush, R. G., S. F. Rice, and T. B. Hunter, "Operation and Performance of the Supercritical Fluids Reactor (SFR)," Tech. Rep. No. SAND96-8203, Sandia National Laboratories, Livermore, CA (1995).

Hart, A. B., J. McFayden, and R. A. Ross, "Solid-Oxide-Catalysed Decomposition of Hydrogen Peroxide Vapour," *Trans. Farad. Soc.*, **59**, 1458 (1963).

Hippler, H., J. Troe, and J. Willner, "Shock Wave Study of the Reaction $HO_2 + HO_2 \rightarrow H_2O_2 + O_2$: Confirmation of a Rate Minimum Near 700 K," *J. Chem. Phys.*, **92**(3), 1755 (1990).

Hirth, T., and E. U. Franck, "Oxidation and Hydrothermolysis of Hydrocarbons in Supercritical Water at High Pressure," *Ber. Bunsenges. Phys. Chem.*, **97,** 1091 (1993).

Hoare, D. E., G. B. Peacock, and G. R. D. Ruxton, "Efficiency of Surfaces in Destroying Hydrogen Peroxide and Hydroperoxyl Radicals," *Trans. Farad. Soc.*, **63,** 2498 (1967).

Holgate, H. R., "Oxidation Chemistry and Kinetics in Supercritical Water: Hydrogen, Carbon Monoxide, and Glucose," PhD Thesis, Dept. of Chemical Engineering, Massachusetts Institute of Technology, Cambridge, MA (1993).

Holgate, H. R., and J. W. Tester, "Oxidation of Hydrogen and Carbon Monoxide in Sub- and Supercritical Water: Reaction Kinetics, Pathways, and Water-Density Effects. 1. Experimental Results," *J. Phys. Chem.*, **98,** 800 (1994a).

Holgate, H. R., and J. W. Tester, "Oxidation of Hydrogen and Carbon Monoxide in Sub- and Supercritical Water: Reaction Kinetics, Pathways, and Water-Density Effects. 2. Elementary Reaction Modeling," *J. Phys. Chem.*, **98,** 810 (1994b).

Japas, M. L., and E. U. Franck, "High Pressure Phase Equilibria and PVT-Data of the Water-Oxygen System Including Water-Air to 673 K and 250 MPa," *Ber. Bunsenges. Phys. Chem.*, **89,** 1268 (1985).

Meyer, E., H. A. Olschewski, J. Troe, and H. Cg. Wagner, "Investigation of N_2H_4 and H_2O_2 Decomposition in Low and High Pressure Shock Waves," *Int. Symp. Combust. Proc.*, published by The Combustion Institute, Pittsburgh, PA, p. 345 (1969).

Michael, J. V., and J. W. Sutherland, "Rate Constant for the Reaction of H with H_2O and OH with H_2 by the Flash Photolysis-Shock Tube Technique over the Temperature Range 1246–2297 K," *J. Phys. Chem.*, **92,** 3853 (1988).

Rice, S. F., T. B. Hunter, Å. C. Rydén, and R. G. Hanush, "Raman Spectroscopic Measurement of Oxidation in Supercritical Water. I. Conversion of Methanol to Formaldehyde," *Ind. Eng. Chem. Res.*, **35**(7), 2161 (1996).

Schmitt, R. G., P. B. Butler, N. E. Bergan, W. J. Pitz, and C. K. Westbrook, "Destruction of Hazardous Waste in Supercritical Water. Part II: A Study of High-pressure Methanol Oxidation Kinetics," 1991 Fall Meeting of the Western States Section/The Combustion Institute, University of California at Los Angeles, p. 19 (1991).

Steeper, R. R., S. F. Rice, I. M. Kennedy, and J. D. Aiken, "Kinetics Measurements of Methane Oxidation in Supercritical Water," *J. Phys. Chem.*, **100,** 184 (1996).

Sutherland, J. W., J. V. Michael, A. N. Pirraglia, F. L. Nesbitt, and R. B. Klemm, "Rate Constant for the Reaction of $O(^3P)$ with H_2 by the Flash Photolysis-Shock Tube and Flash Photolysis-Resonance Fluorescence Techniques; 504 K $\leq$ T $\leq$ 2495 K," *Int. Symp. on Combust. Proc.*, published by The Combustion Institute, Pittsburgh, PA, p. 929 (1986).

Takagi, J., and K. Ishigure, "Thermal Decomposition of Hydrogen Peroxide and Its Effect on Reactor Water Monitoring of Boiling Water Reactors," *Nucl. Sci. Eng.*, **89**, 177 (1985).

Tsang, W., and R. F. Hampson, "Chemical Kinetic Data Base for Combustion Chemistry. Part I. Methane and Related Compounds," *J. Phys. Chem. Ref. Data*, **15**(3), 1087 (1986).

Webley, P. A., and J. W. Tester, "Fundamental Kinetics of Methane Oxidation in Supercritical Water," *Energy & Fuels*, **5**, 411 (1991).

Manuscript received Feb. 10, 1997, and revision received May 12, 1997.